

Design, synthesis and systematic evaluation of all possible cyclic dinucleotides (CDNs) that activate human stimulator of interferon genes (STING) variants

Zheng-Hua Wang^{1†}, Can-Can Zhao^{2†}, Qiang-Zhe Zhang², Chuan-Lin Wang¹, Hang Zhang¹, De-Jun Ma¹, Da-Wei Wang¹, Xin Wen¹, Lu-Yuan Li^{2*} & Zhen Xi^{1,3,4*}

¹State Key Laboratory of Elemento-organic Chemistry, Department of Chemical Biology, College of Chemistry, Nankai University, Tianjin 300071, China;

²State Key Laboratory of Medicinal Chemical Biology and College of Pharmacy, Tianjin Key Laboratory of Molecular Drug Research, Nankai University, Tianjin 300071, China;

³Collaborative Innovation Center of Chemical Science and Engineering (Tianjin), Tianjin 300071, China;

⁴National Pesticide Engineering Research Center (Tianjin), Tianjin 300071, China

Received September 5, 2019; accepted December 13, 2019; published online March 13, 2020

Cyclic dinucleotides (CDNs) are known to activate stimulator of interferon genes (STING) and induce type I interferon responses, therefore possess great potentials to be of immunotherapeutic value for cancers and infectious diseases. However, the existence of different single nucleotide polymorphism (SNP) of human STING (hSTING) gene poses an obstacle to achieve broad-spectrum activation by CDNs. We reported here the design and synthesis of a total of 36 CDNs, representing all structural variations, that contain four bases (A, G, C, U) and two linkage directions (2'-5'-linked and 3'-5'-linked phosphodiester). Through systematic evaluation of IFN- β induction with a dual-luciferase reporter assay, we discovered that wild type hSTING and two isoforms (HAQ and AQ) showed strong response while hSTING-R232H and R293Q exhibited the relatively weak response to CDNs stimulation. For the first time, we found that the c[G(2',5')U(2',5')] showed excellent activity against all five hSTING variants even equivalent to the endogenous ligand c[G(2',5')A(3',5')]. Furthermore, we have also demonstrated that 3'-3' CDNs with two 3'-5' phosphodiester showed higher serum and hydrolase stability than 2'-2' CDNs with two 2'-5' phosphodiester and 2'-3' CDNs with one 2'-5' and one 3'-5' phosphodiester. It is very interesting to note that 2'-2' CDNs has been found for the first time to show strong activity. These findings will stimulate our exploration for the new functional role of CDNs, and provide guidelines to design CDNs based hSTING targeted drugs.

cyclic dinucleotides (CDNs), stimulator of interferon genes (STING), pyrimidine CDNs, interferon β , ecto-nucleotide pyrophosphatase/phosphodiesterase 1 (ENPP1)

Citation: Wang ZH, Zhao CC, Zhang QZ, Wang CL, Zhang H, Ma DJ, Wang DW, Wen X, Li LY, Xi Z. Design, synthesis and systematic evaluation of all possible cyclic dinucleotides (CDNs) that activate human stimulator of interferon genes (STING) variants. *Sci China Chem*, 2020, 63, <https://doi.org/10.1007/s11426-019-9662-5>

1 Introduction

Cyclic dinucleotides (CDNs) have been recognized as im-

portant newly discovered second messengers both in prokaryotes and eukaryotes [1,2]. While double-stranded DNA (dsDNA) as the main stimulator activates cyclic GMP-AMP synthase (cGAS) in the cytoplasm to produce second messenger c[G(2',5')A(3',5')] in metazoan [3–7]. After the synthesis of c[G(2',5')A(3',5')] by cGAS, c[G(2',5')A(3',5')]

[†]These authors contributed equally to this work.

*Corresponding authors (liluyuan@nankai.edu.cn; zhenxi@nankai.edu.cn)

binds and activates the human stimulator of interferon genes (hSTING) proteins to trigger the innate immune signal pathway through the TBK1-IRF3 signal transduction, finally inducing the production of type I interferon (IFN- β) and other pro-inflammatory factors. Besides c[G(2',5')A(3',5')] in mammals, bacterial CDNs including c[G(3',5')G(3',5')], c[A(3',5')A(3',5')] and c[G(3',5')A(3',5')] can also bind and activate STING for the downstream signal transduction [8–11]. There is a growing body of literature that recognizes the importance of CDNs as the new general small molecule drug in immune-therapy. The combination of CDNs with PD-1 antibody [12,13], PD-L1 antibody [14], CAR-T [15], radiation therapeutics [16], and small-molecule drug 5-FU [17], respectively, showed better anti-tumor activity than monotherapy. Recently, two CDN drugs ADU-S100 (NCT02675439, NCT03172936) and MK1454 (NCT03010176) have been approved for the clinical trials for cancer therapy.

Although CDNs act as good candidate of small molecule immune stimulator, the interaction mode of hSTING and CDNs in the structural binding and activation was less understood. Firstly, Kao *et al.* [18] have identified that 57.9% hSTING-WT, 20.4% hSTING-R71H-G230A-R293Q (HAQ), 13.7% hSTING-R232H, 5.2% hSTING-G230A-R293Q (AQ) and 1.5% hSTING-R293Q were distributed in the human populations. These single nucleotide polymorphisms (SNPs) in hSTING have been shown different responses to bacterial CDNs [18]. The categories of CDNs targeting all the hSTING variants were relatively rare, and it would be very interesting to explore the structural varieties of CDNs to gain the wide spectrum activators with high potency. Recently, Kranzusch *et al.* [19] found that bacterial cGAS/DncV like nucleotidyltransferases (CD-NTases) could synthesize pyrimidine CDNs. But these CDNs could not activate the mouse STING (mSTING) dependent type I interferon signaling in mammalian cells. However, all of these reported CDNs with pyrimidine bases were linked by two 3'-5' phosphodiester bonds, which was different from CDNs linked with a non-canonical 2'-5' phosphodiester bond in mammal cells [11,19]. The linkage mode might regulate the different signal pathway for diverse functions in cells. Hence, a systematic evaluation of all possible CDNs including four bases (A, G, C, U bases) and two linkage directions (2'-5'-linked phosphodiester and 3'-5'-linked phosphodiester) against all the reported hSTING variants was necessary to establish the relationship of the structure and activity. These understanding on the interaction mode of CDNs and hSTING variants will help us to find efficient hSTING activators with good serum stability.

In this article, we reported the synthesis and biological activity of CDNs with all the possible combination of A, U, C, G bases and 2'-5' and 3'-5' phosphodiester linkages (Figure 1). The CDNs and its analogs were obtained through

phosphotriester-approach. The name of CDNs followed the principle as shown in Figure 1. The activity of IFN- β induction on wild type hSTING and isoforms was obtained through dual-luciferase assays. Furthermore, both of the serum and ecto-nucleotide pyrophosphatase/phosphodiesterase 1 (ENPP1) hydrolase stability of CDNs were also studied.

2 Experimental

2.1 Chemical materials, general procedures, and methods

All solvents and reagents were purchased from commercial sources and used without further purification. The reaction was monitored by thin layer chromatography (TLC) on silica gel GF254 with detection under UV light. Nuclear magnetic resonance spectroscopy (NMR) spectra were recorded on Bruker AVANCE 400M (Germany) instrument at 298 K. Chemical shifts were relative to tetramethylsilane (TMS) (0.00). The following abbreviations were used to explain the multiplicities: s (singlet), d (doublet), t (triplet), q (quartet), m (multiplet). The number of protons (n) for a given resonance was indicated as n H. High resolution mass spectrum (HRMS) (MALDI-TOF) was obtained from Varian 7.0T FTMS (USA). UPLC-HRMS (ESI) spectra were recorded on Waters Xevo G2-XS Q-TOF mass spectrometry (USA). HPLC was achieved using Agilent 1260 (USA). Preparative column with an ASB C18 column (10 μ m, 21.2 mm (diameter) \times 250 mm (height)) (Agela Technologies) and the preparative LC with Agela OCTOPUS purification System were used. 1 M triethylammonium bicarbonate (TEAB) buffer was prepared by bubbling CO₂ through a 1 M Et₃N solution in H₂O until pH~8.5. 1 M triethylamine acetate (TEAA) buffer was prepared by adding CH₃COOH to Et₃N in water until pH 7.0 and then filtering through a 0.45 μ m membrane filter. Both TEAA and TEAB buffer were kept in 4 $^{\circ}$ C.

2.2 Biological materials and general procedures

HEK293T and THP-1-lucia cells were maintained in culture

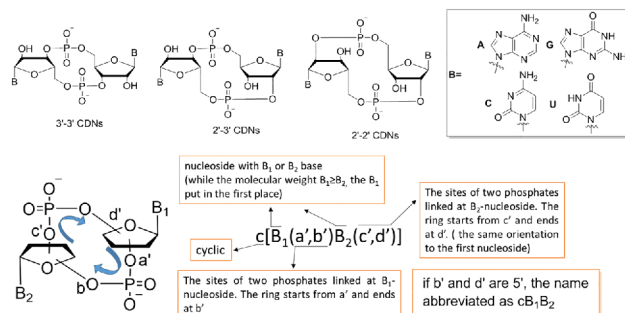


Figure 1 General structure of CDNs with different bases, phosphodiester linkage and the name principle of CDNs (color online).

medium (DMEM and RPMI 1640, separately) supplemented with 10% fetal bovine serum (FBS) and 1% penicillin/streptomycin under the condition of 37 °C and 5% CO₂. The biological materials were purchased from the corresponding commercial sources and used as received: Anti-TMEM173 (hSTING) antibody [EPR13130] (Abcam, ab181125), Anti-GAPDH mouse monoclonal antibody (CW BIO, CW0100M), Goat-anti-mouse IgG HRP-conjugated (CW BIO, CW0102S), Goat-anti-Rabbit IgG HRP-conjugated (CW BIO, CW0103S), Recombinant Human ENPP1 protein (R&D, 6136-EN-010), Digitonin (Abcam, ab141501), DMXAA (MCE, HY-10964), Polyjet (Signagen, SL100688), FBS-Australian Origin (Life, 10099-141), ECL reagent (GE Healthcare), Dual-Luciferase[®] Reporter Assay System (Promega, E1960), TRIZON Reagent (CW BIO, CW0580S).

2.3 Plasmid constructions

The pGL3-IFN- β plasmid was a gift from prof. Nicolas Mannel (Addgene 102597) [20]. The pGL4.74-Rluc-TK plasmid was purchased from Promega (E6921). The full-length hSTING-WT gene sequence was synthesized by AuGCT DNA-SYN Biotechnology Company (Beijing, China) and cloned into pcDNA3.1 plasmids vector. pcDNA3.1-hSTING-R232H, pcDNA-hSTING-HAQ, pcDNA3.1-hSTING-AQ, and pcDNA3.1-hSTING-R293Q plasmids were constructed by site-directed mutagenesis method using the polymerase chain reaction (PCR). The primers were shown in Table S1 (Supporting Information online). The gene sequence encoding the C-terminal domain (CTD) of hSTING (aa 139-379) was inserted into the pET28b(+) vector between NdeI and XhoI sites, resulting N-terminal and C-terminal hexahistidine tag. Mutants were generated by site-directed mutation through PCR using the pET28b(+)-hSTING-WT vector as the template and confirmed by sequencing.

2.4 Dual-luciferase reporter assay

5 \times 10⁴ HEK293T cells were seeded in 24-well plates. pcDNA3.1-hSTING (50 ng), pGL3-IFN β (firefly) (400 ng), and pGL4.74-Rluc-TK (renilla) (50 ng) were co-transfected. After 12 h, cells were stimulated with CDNs (5 μ M) using digitonin permeabilization (50 mM *N*-2-hydroxyethylpiperazine-*N*-2-ethane sulfonic acid (HEPES), 100 mM KCl, 3 mM MgCl₂, 0.1 mM dithiothreitol (DTT), 85 mM sucrose, 0.2% bovine serum albumin (BSA), 1 mM adenosine triphosphate (ATP), 0.1 mM GTP, and 10 μ g/mL digitonin) [21]. After 30 min, the stimulation mixture was removed and the normal media was added. After 12 h, cell lysates were prepared and the relative luciferase activity between the Firefly luciferase and the Renilla luciferase was measured using the dual-luciferase reporter assay system.

2.5 In vitro stability assay in serum and ENPP1 solutions

Each CDNs (0.1 μ g/mL) was incubated in either a ENPP1 solutions (30 μ L) containing 2 nM ENPP1, 2 mM Ca²⁺, 0.2 mM Zn²⁺, 20 mM Tris-HCl pH 9.0, 0.2% NP-40; or 20% FBS, 20 mM PBS pH 7.4, 5 mM Mg²⁺ or in water (as the negative control) at 37 °C. At various time, aliquots of the reaction mixture was collected and stopped by adding 5 μ L EDTA (0.5 M, pH 8.0) and diluted with 80 μ L water. The reaction mixture was then centrifuged at 10,000 r/min for 10 min, leaving the 100 μ L supernatant for the high performance liquid chromatography (HPLC) assay. 20 μ L of each aliquot was injected directly into HPLC (Agilent 1260 Infinity HPLC equipped with a UV detector; column Agilent ZORBAX SB-C18 5 μ m (4.6 \times 150 mm); detection at 254 nm; column temperature: 25 °C) for analysis. 10 mM TEAA buffer (solvent A) and MeCN (solvent B) were used as the mobile phase with a flow rate of 1 mL/min. The gradient was set as following: 0–2 min: 100% A; 2–12 min: 100% A to 80% A/0% B to 20% B; 12–13.5 min: 80% A to 0% A/20% B to 100% B; 13.5–15 min: 100% B; 15–17 min: 0% A to 100% A/100% B to 0% B.

2.6 Molecular dynamics simulations

We carried out a investigation on the equilibrium conformations of hSTING in the presence and absence of ligands by molecular dynamics simulations using Amber 14 molecular modelling package [22,23]. The X-ray structure of hSTING was retrieved from the Protein Data Bank (PDB code: 4F5D). Ala230 in the crystal structure of hSTING cytoplasmic domain was mutated back to the wild type residues Gly230. Amber ff14SB force field [24] was used to parameterize amino acids residues of hSTING. The force field parameters of CDNs come from previous work [25]. Each system was immersed in a truncated octahedral box of explicit TIP3P water molecules. Particle Mesh Ewald (PME) [26] and periodic boundary condition was employed to deal with the long-range electrostatic interactions. SHAKE method [27] was used to constrain bonds involving hydrogen atoms in order to tolerate a time step of 2 fs. The system was gradually heated from 0 to 300 K over 50 ps. The equilibrating calculation was executed at 1 atm and at 300 K for 50 ps. Then, 15 ns MD simulations were performed under 300 K and 1 atm. The snapshot of the system was taken every 1 ps.

2.7 Docking calculations of c[G(2',5')U(2',5')] and hSTING-R232H

The structure of hSTING-R232H (aa 139-379) (PDB ID: 4LOH) was download from PDB, the water molecules and

the ligand in the crystal structure were removed by PyMol. c[G(2',5')U(2',5')] was constructed by SYBYL-X 2.0 (Tripos, Inc., USA) and subsequently optimized with the conjugate-gradient and steepest-descent algorithm to a convergence criterion of 0.005 kcal/mol. The parameters were prepared by standard methods using Autodock Tools Package before docking. Docking calculations of receptor and ligands were performed on AutoDock 4.2. For each ligand, the docking runs were set to 200. After calculation, the results were clustered, and the best binding modes were selected by the docking energy as well as by comparison with the reference co-crystal ligand.

2.8 Protein expression and purification

All proteins were expressed in *E. coli* BL21(DE3) and induced with 0.5 mM isopropyl- β -D-1-thiogalactopyranoside (IPTG) when OD600 reached 0.5–0.6 and grew overnight at 20 °C. Cells were spun down and lysed in lysis buffer (20 mM Tris-HCl pH 7.5, 300 mM NaCl, 20 mM imidazole). After centrifugation and removal of cell debris, supernatant was incubated with Ni-NTA beads. Ni-beads were washed extensively and protein was eluted in wash buffer (20 mM Tris-HCl pH 7.5, 300 mM NaCl, 300 mM imidazole). Eluted protein was further cleaned by GE Disposable PD-10 columns in assay buffer (20 mM Tris-HCl pH 7.5, 150 mM NaCl). Proteins were flash frozen in liquid nitrogen and stored at –80 °C.

2.9 Isothermal titration calorimetry

The thermodynamic parameters of binding reactions of hSTING-CTD with CDNs were measured by isothermal titration calorimetry using a PEAQ-ITC (Malvern) at 25 °C.

2.10 IFN- β induction in THP-1-luciferase cells

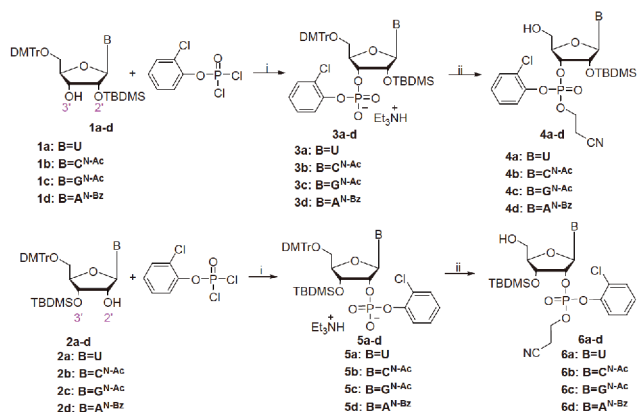
5×10^5 THP-1-luciferase cells were seeded in 24-well plate. 10 μ M CDNs were dissolved in the culture media directly without any transfection reagent. After stimulation with 24 h, the luciferase were measured for the IFN- β induction.

3 Results and discussion

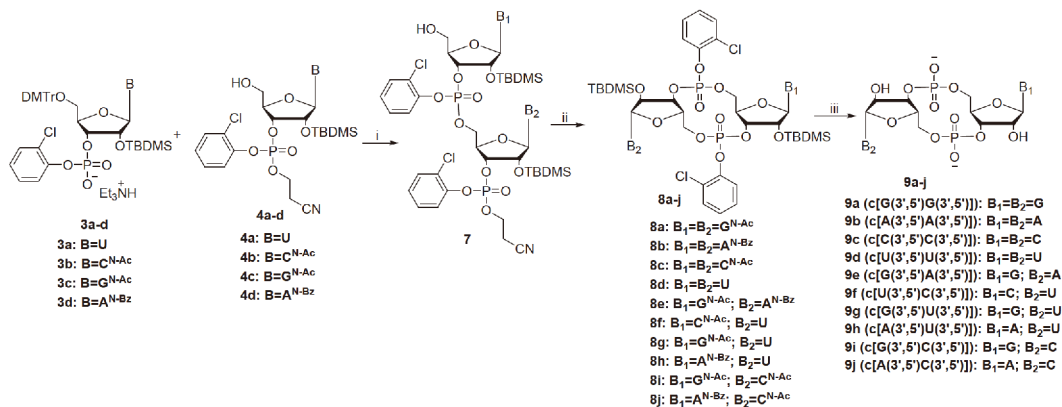
3.1 Synthesis of CDNs

All possible CDNs including two phosphodiester linkage bonds (2'-5' and 3'-5') and four bases (A, G, U, C) were synthesized through the phosphotriester approach. Firstly, 2-chlorophenyl phosphorodichloridate was chosen as phosphorylation reagent and was introduced onto the 3'-OH or 2'-OH of the nucleosides **1a–1d** and **2a–2d** to get the first building blocks **3a–3d** and **5a–5d** (Scheme 1). The second

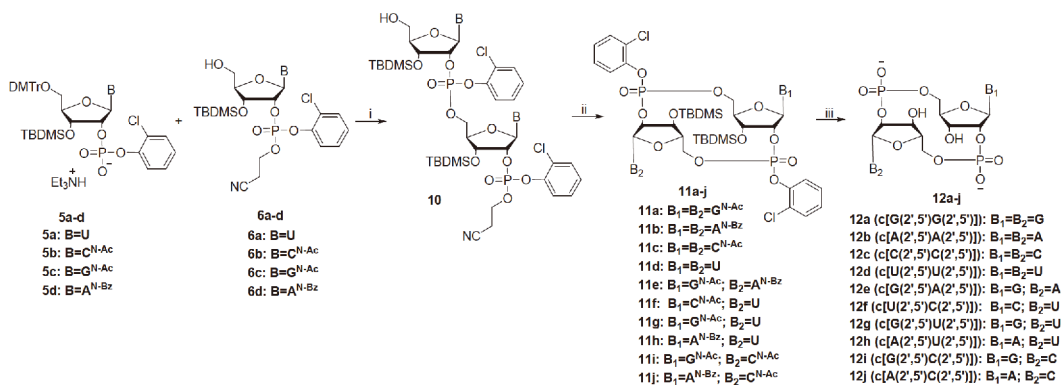
protecting group of phosphate was then introduced with the 3-hydroxypropionitrile. The two different protecting groups could be removed under mild conditions. After the 5'-OH protecting group DMTr was removed in a solution of 3% dichloroacetic acid (DCA) in dichloromethane, the second building blocks **4a–4d** and **6a–6d** were obtained. As shown in Scheme 2, the coupling reactions of 5'-O-DMTr-2'-O-TBDMS-3'-phosphodiester nucleotides **3a–3d** with 5'-OH-2'-O-TBDMS-3'-phosphotriester nucleotides **4a–4d** were achieved in the presence of 1-(2-mesitylenesulfonyl)-3-nitro-1H-1,2,4-triazole (MSNT) in anhydrous pyridine to form linear dimeric nucleotide **7** following the elimination of 5'-DMTr under the acidic condition. When the linear intermediates were obtained, phosphate protecting groups were removed under *t*BuNH₂-MeCN mixture and the cyclization was achieved with the help of the coupling reagent MSNT in anhydrous pyridine to obtain the fully protected cyclic dinucleotides **8a–8j**, which were subsequently treated with N1, N1,N3,N3-tetramethylguanidinium (TMG) and *syn*-pyridine-2-carboxaldoximate (PBO) complex in water and 1,4-dioxane solution to remove the 2-chlorophenyl groups. In the following step, the base protection with benzoyl and acetyl groups were removed in 33 wt% MeNH₂-EtOH solution and *tert*-butyldimethylsilyl (TBDMS) groups were removed using Et₃N•3HF mixture. The 3'-3' CDNs with two 3'-5' phosphodiester linkages **9a–9j** were achieved with preparative RP-HPLC. As shown in Scheme 3, the 2'-2' CDNs with two 2'-5' phosphodiester linkages **12a–12j** were obtained through the coupling reaction of the 2'-O-TBDMS-3'-phosphorylated building blocks **5a–5d** with **6a–6d** followed by the same cyclization and deprotection steps. The combination of 3'-O-TBDMS-2'-phosphorylated intermediates **3a–3d** with 2'-O-TBDMS-3'-phosphorylated intermediates **6a–6d** or intermediates **4a–4d** with **5a–5d** resulted in the formation of 2'-3' CDNs with one 3'-5' phosphodiester linkage and one 2'-5' phosphodiester linkage **16a–16p** (Scheme 4). In summary,



Scheme 1 Synthesis of intermediates **3a–3d**, **4a–4d**, **5a–5d**, **6a–6d**. Reagents and conditions: (i) 1) 1,2,4-triazole, Et₃N, CH₂Cl₂; 2) TEAB buffer; (ii) 1) 3-hydroxypropionitrile, MSNT, pyridine; 2) 3% DCA, CH₂Cl₂ (color online).



Scheme 2 Synthesis of 3'-3' CDNs **9a–9j**. Reagents and conditions: (i) 1) MSNT, pyridine; 2) DCA, CH₂Cl₂; (ii) 1) *t*BuNH₂, MeCN; 2) MSNT, pyridine; (iii) 1) TMG, PBO, 1,4-dioxane, H₂O; 2) MeNH₂, EtOH; 3) pyridine, Et₃N, Et₃N·3HF.



Scheme 3 Synthesis of 2'-2' CDNs **12a–12j**. Reagents and conditions: (i) 1) MSNT, pyridine; 2) DCA, CH₂Cl₂; (ii) 1) *t*BuNH₂, MeCN; 2) MSNT, pyridine; (iii) 1) TMG, PBO, 1,4-dioxane, H₂O; 2) MeNH₂, EtOH; 3) pyridine, Et₃N, Et₃N·3HF.

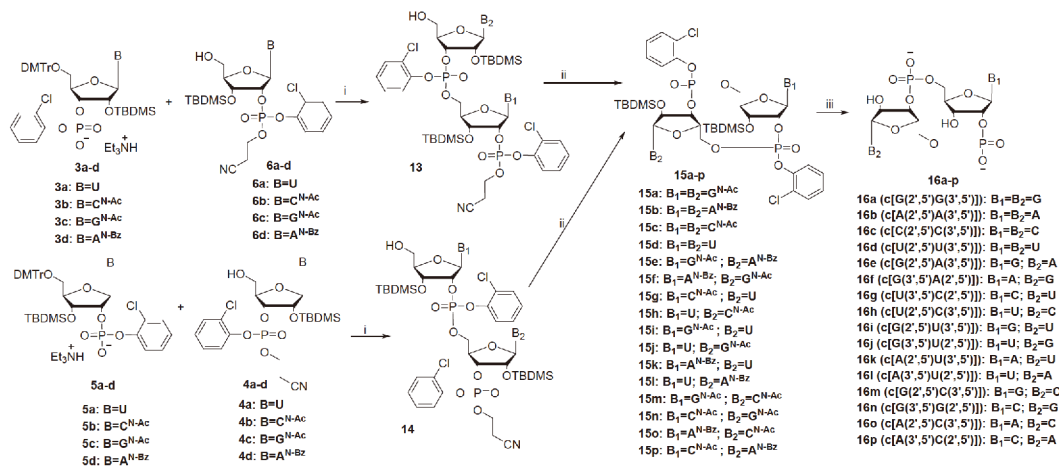
36 analogues of CDNs (**9a–9j**, **12a–12j**, and **16a–16p**) with different bases and different phosphodiester linkage combinations were successfully synthesized and characterized.

3.2 IFN- β luciferase induction through activating wild type hSTING and its SNPs elicited by CDNs

After the stimulation of CDNs, STING recruits TBK1 kinase to induce the phosphorylation of the transcription factor IRF3, which subsequently dimerizes and translocates into the nucleus and binds IFN- β promoter to induce the production of type I interferons [28–30]. Based on this principle, IRF3-responsive dual-luciferase reporter assay was established to determine the activity in IFN- β activation [5,20,31]. Herein, we determined the activity of 36 CDNs through the IRF3-binding induced fluorescence increase when dual-luciferase reporter vectors and hSTING expressing vectors were co-transfected into HEK293T cell.

To compare the sensitivity of hSTING variants to all these CDNs, we firstly introduced five hSTING variants containing different SNPs (WT, HAQ, AQ, R232H, R293Q) in the expressing vectors [18], which was confirmed by Sanger sequencing (Figure S1, Supporting Information online). In

the presence of hSTING-expressing plasmids, reporter plasmids pGL3-IFN β (firefly) and pGL4.74-Rluc-TK (renilla) were also co-transfected into HEK293T cells and incubated for 12 h. The transfection of CDNs needs the help of digitonin permeabilization [21,32]. After the cell lysis, all five hSTING proteins could be detected by immune blotting but no endogenous hSTING proteins were observed, indicating the over-expression of exogenous hSTING proteins in cells (Figure S1). As shown in Figure 2, in the absence of CDNs, the transfection of different hSTING-expressing plasmids (50 ng/well) exhibited different activity to activate IFN- β pathway. The relative activity was ranked as follows: R232H (12.2 fold)>WT (8.3 fold)>HAQ (3.8 fold)>R293Q (2.3 fold)>AQ (1.0 fold). When the endogenous ligand **16e** (c[G(2',5')A(3',5')]) was added, all five hSTING proteins responded to **16e** differently with the following ranking activity: AQ (66.9 fold)>R293Q (49.6 fold)>HAQ (18.4 fold)>WT (14.9 fold)>R232H (8.3 fold) although the overall activity was upregulated for all hSTING proteins compared with the cells only transfected hSTING expression plasmids. Among five hSTING proteins, **16e** exerted the greatest activation to hSTING-AQ, indicating the possible strong interaction between **16e** and hSTING-AQ. The results



Scheme 4 Synthesis of 2'-3' CDNs **16a–16p**. Reagents and conditions: (i) 1) MSNT, pyridine; 2) DCA, CH₂Cl₂; (ii) 1) *t*BuNH₂, MeCN; 2) MSNT, pyridine; (iii) 1) TMG, PBO, 1,4-dioxane, H₂O; 2) MeNH₂, EtOH; 3) pyridine, Et₃N, Et₃N·3HF.

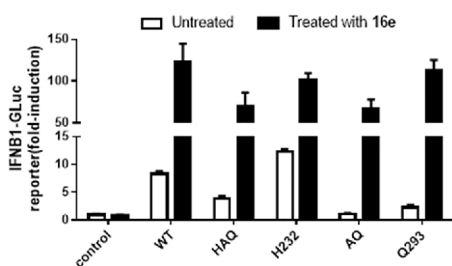


Figure 2 IFN- β luciferase induction activity of WT hSTING and SNPs with or without stimulated with **16e** (5 μ M) for 12 h in HEK293T cells. Data were presented as mean \pm s.e.m; $n=5$.

demonstrated the feasibility of using IRF3 responsive dual-luciferase reporter assay to evaluate the potency of CDNs.

We further evaluated the activity of 3'-3' CDNs with two 3'-5' phosphodiester linkage (**9a–9j**). As shown in **Figure 3**, only bacterial CDNs such as **9a** (c[G(3',5')G(3',5')]), **9b** (c[A(3',5')A(3',5')]) and **9e** (c[G(3',5')A(3',5')]) could activate hSTING-WT and hSTING-AQ. The introduction of U and (or) C base did not trigger hSTING-dependent IRF pathway. In contrast with hSTING-WT, hSTING-HAQ was less sensitive to **9a** (**Figure 3(c)**) while hSTING-R232H showed much weaker response to **9a** and **9e**. Interestingly, the mutation of R232H nearly abolished its response to **9b**, which revealed the important role of Arg232 in binding **9b** (**Figure 3(d)**). Among all the 3'-3'CDNs, only **9e** could effectively activate five hSTING variants, which might be a broad-spectrum hSTING activator.

Subsequently, we evaluated the activity of 2'-2' CDNs with two 2'-5' phosphodiester linkage (**12a–12j**) (**Figure 4**). The results showed that 2'-2' CDNs with two purine rings could activate hSTING-WT, hSTING-HAQ and hSTING-AQ variants while showing low activation to hSTING-R232H and R293Q variants. **12e** (c[G(2',5')A(2',5')]) also showed good activities to all five mutants, except much lower to R232H. Unlike 3'-3' CDNs, 2'-2' CDNs with mixed pyr-

imidine ring recovered their activity like **12d** c[U(2',5')U(2',5')], **12g** (c[G(2',5')U(2',5')]), and **12i** (c[G(2',5')C(2',5')]) targeting hSTING-WT and hSTING-AQ. **12d** failed to activate hSTING-HAQ. Among all the 2'-2' CDNs (**12a–12j**), interestingly, only **12g** was observed to activate all the five hSTING variants. What is more, the **12g** (106.2 fold) had higher ability to activate hSTING-AQ than **16e** (87.1 fold).

Finally, the activity of 2'-3' CDNs (**16a–16p**) was also evaluated (**Figure 5**). We found that CDNs with two purine bases containing one 2'-5' phosphodiester and one 3'-5' phosphodiester bond could induce robust activation to hSTING-WT, hSTING-HAQ, and hSTING-AQ proteins. **16f** (c[G(3',5')A(2',5')]) decreased the capacity of activating hSTING-R232H and hSTING-R293Q. **16a** failed to activate hSTING-R293Q. Similarly, 2'-3' CDNs with mixed pyrimidines like **16g** (c[U(3',5')C(2',5')]), **16i** (c[G(2',5')U(3',5')]), **16j** (c[G(3',5')U(2',5')]), **16l** (c[A(3',5')U(2',5')]) and **16p** (c[A(3',5')C(2',5')]) also activated hSTING-WT and hSTING-AQ but failed to activate hSTING-R232H and hSTING-R293Q. Only **16i** and **16j** could partly activate hSTING-HAQ. Among all the 2'-3' CDNs (**16a–16j**), only **16e** could effectively activate five hSTING variants.

Previous studies have confirmed that the purine rings G and A could easily be able to stack with Tyr167 and Arg238 of hSTING, which made the CDNs with GG, AA, and GA showing excellent activity to activate hSTING immune pathway [32]. Comparing the activity of 3'-3' CDNs, 2'-2' CDNs, and 2'-3' CDNs, we found that all the CDNs with purine bases (A and G) showed good activity to induce IFN- β luciferase production as expected. The CDNs constructed with G and A bases, like **9e**, **12e**, **16e**, and **16f**, exhibited relative strong activities to all five hSTING variants. And what is more, the metazoan ligand **16e** was the strongest hSTING activator. It was taken for granted that hSTING should not sense CDNs with mixed pyrimidine bases be-

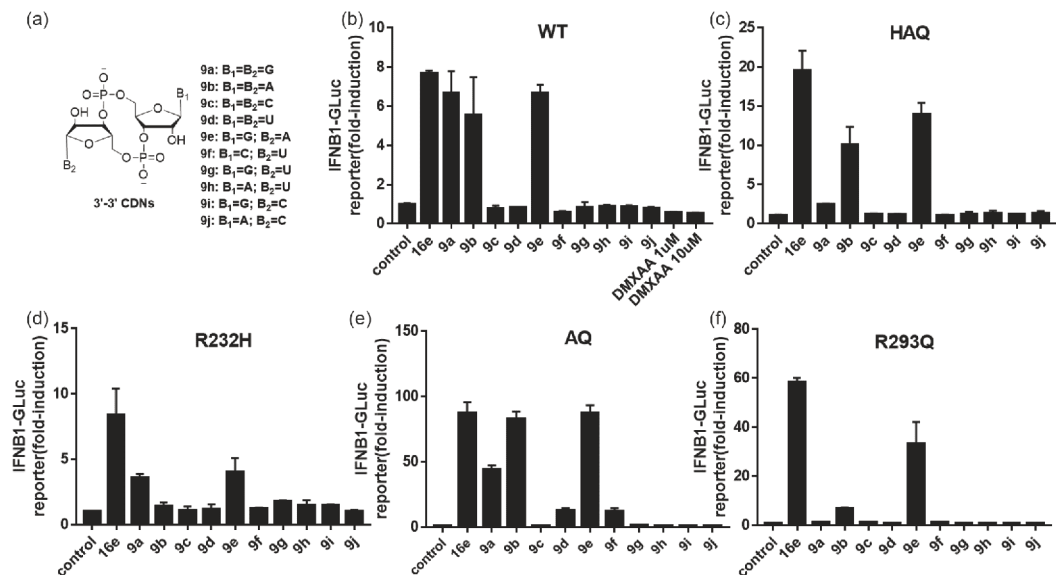


Figure 3 The activity of 3'-3' CDNs against five hSTING variants. (a) The general structure of 3'-3' CDNs; (b–f) HEK293T cells were cotransfected with IFN-β-luciferase reporter plasmids and the test plasmids expressing (b) hSTING-WT, (c) hSTING-HAQ, (d) hSTING-R232H, (e) hSTING-AQ, and (f) hSTING-R293Q. After 24 h, cells were further stimulated for 12 h in the presence of CDNs (5 μM) and then used for the luciferase assay. Data were presented as mean±s.e.m; *n*=5.

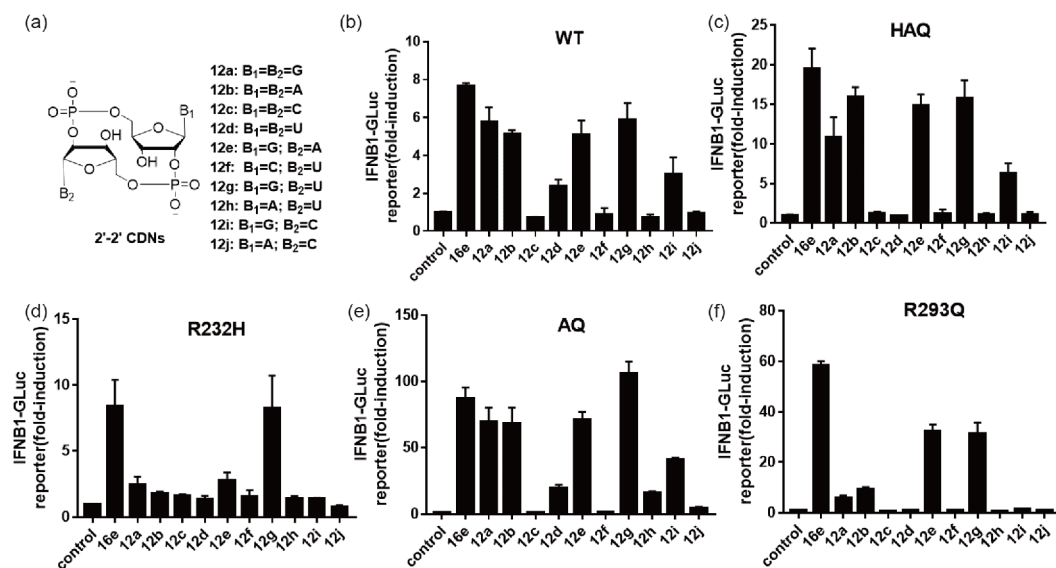


Figure 4 The activity of 2'-2' CDNs against five hSTING variants. (a) The general structure of 2'-2' CDNs; (b–d) HEK293T cells were cotransfected with IFN-β-luciferase reporter plasmids and the test plasmids expressing (b) hSTING-WT, (c) hSTING-HAQ, (d) hSTING-R232H, (e) hSTING-AQ, and (f) hSTING-R293Q. After 24 h, cells were further stimulated for 12 h in the presence of CDNs (5 μM) and then used for the luciferase assay. Data were presented as mean±s.e.m; *n*=5.

cause the pyrimidine ring would not be able to reach Tyr167 for the favorable stacking interaction [32]. Surprisingly, we have found here that CDNs with mixed pyrimidine bases **12d**, **12g**, **12i**, **16g**, **16i**, **16j**, **16l**, and **16p** could activate hSTING, in which **12g** showed as same if not better activity as CDNs with purine bases, and **12g** exhibited excellent activity to all the five hSTING variants. As we found, all the CDNs with mixed pyrimidines containing at least one 2'-5' linkage bond stimulated the IFN-β induction. The 2'-5'

linked phosphate group have a higher propensity than 3'-5' linked phosphate to form hydrogen bonding with Arg232 [33], which might also provide the explanation that hSTING-R232H responded poorly to the majority of CDNs.

When hSTING expression plasmids were transfected into HEK293T cells, the IFN-β Luc reporter was also induced without stimulation of CDNs. We hypothesized this phenomenon may be caused by the hSTING self-activation. hSTING self-activation was more obviously in some gain-

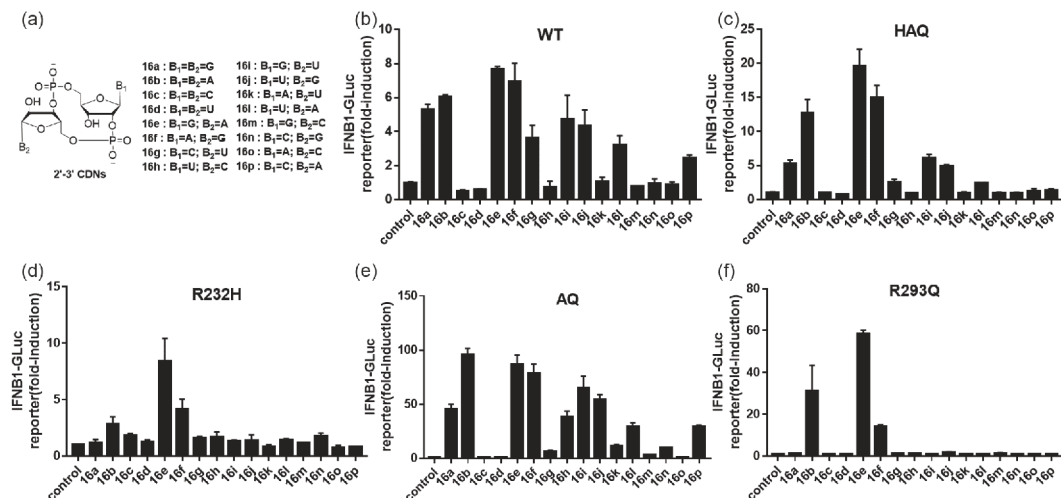


Figure 5 The activity of 2'-3' CDNs against five hSTING variants. (a) The general structure of 2'-3' CDNs; (b–f) HEK293T cells were cotransfected with IFN- β -luciferase reporter plasmids and the test plasmids expressing (b) hSTING-WT, (c) hSTING-HAQ, (d) hSTING-R232H, (e) hSTING-AQ, and (f) hSTING-R293Q. After 24 h, cells were further stimulated for 12 h in the presence of CDNs (5 μ M) and then used for the luciferase assay. Data were presented as mean \pm s.e.m; $n=5$.

of-function mutations like R248S, R281Q, R284G, V155M, N154S, etc, which were found in autoimmune disease patients called STING-associated vasculopathy with onset in infancy (SAVI) [34–37]. Without the stimulation of CDNs, these patients showed higher level of IFN- β than healthy people. Depending on the general understanding of hSTING-activation mode, when hSTING bound to CDNs, the two protomers of hSTING will shift closely. As a result, the hSTING was changed from an “open” conformation to a “closed” conformation [5,6]. Thus, the degree of “opening” or “closing” of the two arms of the V-shaped hSTING dimer was evaluated here by the distance between two Thr181-C α from each hSTING protomer. Depending on the reported structures of apo-hSTING and hSTING-CDNs complexes, the distances were distributed in a range of 33.77–48.33 Å (Figure S2) [5,32,38–42]. We defined the distance distributed in a range of 33.77 \pm 1 Å as the active conformation of hSTING. Molecular dynamics simulations for hSTING in the presence and absence of CDNs were carried out to generate the equilibrium conformations with Amber14 software. The probability of active conformation was calculated. The results were shown in Table 1 and Figure S3. The probability distribution of apo-hSTING, 16e-hSTING, and 9a-hSTING were 0.13, 0.56, and 0.58, respectively. It indicated that without any ligands, the apo-hSTING could also form the active conformation by itself with a certain probability. This means that the hSTING protein could be activated and induce downstream signaling transduction pathway without the stimulation of ligands. The Western Blot results indicated that the expression level of each hSTING variants were similar (Figure S1) [18,31], but the ability of self-activation or CDNs-mediated activation were much different. And the sensitively of each hSTING iso-

Table 1 Dynamic data distributed in the range of 33.77 \pm 1 Å

	Apo-hSTING	16e-hSTING	9a-hSTING
Amounts of active conformation	1,728	7,281	7,537
Possibility of active conformation	0.13	0.56	0.58

forms response to 16e were also much different. The hSTING-AQ had the lowest activity without the stimulation of 16e, but it was most sensitive to 16e.

All five hSTING variants showed different response to 36 CDNs, indicating the interaction complexity between CDNs and hSTING proteins. The hSTING is ER-membrane located protein, which makes it difficult to achieve the full-length crystal structure for the study of hSTING-CDNs binding mode before. Fortunately, the cryo-EM structure of full-length hSTING (PDB: 6NT5) has been dissolved [41]. According to the apo-hSTING full-length structure, Arg71 site was located between the transmembrane helix α 2 and helix α 3 of the N-terminus and the Arg293 site was located on the helix α 3 of CDN binding domain (CBD) of hSTING contacting with the transmembrane domains and forming charge-charge interaction with Glu149 and Arg76 (Figure 6 (a, b)) [41]. Both of two sites had no direct contact with ligands but might help stabilize the dimerization of hSTING. Resulting in the mutations of R293Q or R71H interfered with the translocation or aggregation of hSTING to initiate the IFN- β pathway. It might be more important for R293Q mutation to affect the rotation of each hSTING protomer induced by CDN binding [41].

Furthermore, there were two sites affecting the CDNs binding like Gly230 and Arg232 sites located in the highly flexible loop region between β 2 and β 3 strands of hSTING

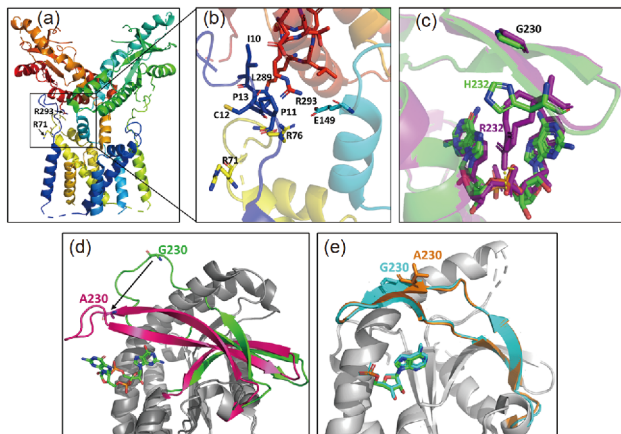


Figure 6 Comparison of the structure of hSTING SNP variants. (a) Full length of apo-hSTING-WT (PDB: 6NT5). (b) Close view of Arg71 and Arg293 sites located in apo-hSTING-WT (PDB: 6NT5). (c) Comparison of the structure changes when **16e** bound to hSTING-WT (PDB:4KSY, magenta) and hSTING-H232 (PDB:4LOH). (d) Comparison of the lip region change when **9a** bound to hSTING-WT (PDB:4F5Y, green) and hSTING-G230A (PDB:4F5D, hotpink). (e) Comparison of the structure changes when **9b** bound to hSTING-WT (PDB:6CFF, cyan) and hSTING-G230A (PDB:6CYT, orange) (color online).

protein. When CDNs bound to hSTING, this flexible loop region would transform into four β -sheets covering on top of the binding-pocket [6], which would increase the binding affinity of hSTING protein to CDNs. It could be well validated that the loop region in hSTING-WT did not form the ordered β -sheet [39] but the loop region in hSTING-G230A formed the ordered sheet when bound by **9a** (Figure 6(d)) [38]. However, there was no obvious difference between hSTING-WT and G230A when bound by **9b** (Figure 6(e)) [43]. Since G230A mutated hSTING favored the closed conformation in the presence of some CDNs [18], hSTING-HAQ and hSTING-AQ were largely sensitive in response to different CDNs (Figure 6(c)). For Arg232 mutation, we took the crystal complex of **16e** and hSTING-WT (PDB:4KSY) as the example [6], and found that the two phosphate groups could form hydrogen bonding with Arg232, which was absent in the crystal complex of **16e** and hSTING-R232H (PDB: 4LOH) [5]. It revealed that the R232H mutation decreased the activation of hSTING and provided an explanation of the weak activation to hSTING-R232H by the majority of CDNs in our hands. We also recorded the isothermal titration calorimetric (ITC) binding curves for the complex formation of hSTING-WT, R232H and AQ variants C-terminal domain (CTD) (aa 139–379) with **9a**, **9e** and **16e** as shown in Figure S13 and the ITC-based thermodynamic parameters as shown in Table S2. K_d value of the complexes formation of **16e** and **9e** to hSTING-WT-CTD were 5.91 nM and 1.59 μ M, separately. But while **16e** and **9e** bound to hSTING-R232H-CTD, the K_d value were dramatically increased (3.33 and 5.44 μ M, separately). It indicated the binding affinity was decreased while CDNs bind to R232H

mutant. But there was no much different while **9a** bound to hSTING-WT and R232H CTD (2.82 and 2.84 μ M). As previous reported, while **9a** bound to hSTING-WT-CTD, the K_d value was two-fold compared to the hSTING-G230A-CTD [18]. When **9a** bound to hSTING-AQ-CTD, the K_d value was also half (1.26 μ M) compared to hSTING-WT-CTD. It indicated that the R293Q mutation has low influence to the binding affinity of CDNs to hSTING-CTD. So depending on the structure and bioactivity data analysis, we forecasted that the R71H, R232H, and R293Q were loss-of-function mutations, but the G230A was a kind of gain-of-function mutation. But all of these mutations did not affect the responses to the metazoan ligand **16e** and the synthetic ligand **12g**.

The previous study explored that the purine rings would have more potency to form stacking interactions with Arg238 and Tyr167 of hSTING than pyrimidine rings [6]. As shown in Figure S5, when **9a** bind to hSTING (PDB: 4F5D), the G1 base would have potency to form stacking with A_Tyr167 (Tyr167 residue located in hSTING protomer A) and B_Arg238 (Arg238 residue located in hSTING protomer B), and the interactions we labeled as Π_1 and Π_2 , separately. The G2 ring could form stacking with B_Tyr167 and A_Arg238, and the interactions were also labeled as Π_3 and Π_4 , separately (Figure S5). Here, we calculated the stacking interactions between the bases of CDNs like **9a**, **9b**, **9c**, **9d**, **9e**, and **16e** with hSTING Tyr167 and Arg238 residues. We got all of the data after 2 ns (Figures S6–S11). We counted the data distributed in the range of 0–20° dihedral angle and 3.4–4 Å distance. As shown in Table 2, the purine rings have more potency to form stacking interactions than pyrimidine rings, especially the interaction with Arg238 residues. These results further supported the idea that CDNs with purines would have a higher binding affinity with hSTING. The two U rings of **9d** also showed favored stacking interaction with Arg238 and Tyr167. But when the **9c** bind to hSTING, only one C ring could form stacking with Arg238 and Tyr167. The U ring was more favored to stack with Tyr167 and Arg238 than C ring. It indicated that CDNs with pyrimidines, especially the U rings could also bind to hSTING with a certain binding affinity. However, the **9d** only showed limited activity to activated hSTING-AQ (12.8 fold) (Figure 3(e)). While for pyrimidine CDNs contained 2'-5' phosphodiester linkage, their ability to activate hSTING was increased (Figures 4, 5 and S4). Except for the **9g**, CDNs with G and U bases combination (**12g**, **16i**, and **16j**) could activate hSTING-WT, hSTING-AQ, and hSTING-HAQ with higher activity than other pyrimidine CDNs (Figure S4). Furthermore, **12g** also showed good activity to induce IFN- β Luciferase production mediated by hSTING-R232H and R293Q isoforms.

Since we found several CDNs had excellent ability to activate all five hSTING isoforms like **12g** and **16e**, we

further investigated the mechanism of the broad-spectrum activity based on the binding mode of **12g** and hSTING-R232H (PDB:4LOH) [5] through the docking calculations which was performed on AutoDock 4.2. When **12g** bound to hSTING-R232H protein, **12g** showed a similar conformation to **16e** in that the uracil group forms the same stacking with Arg238 and Tyr167 (Figure 7(a, c)). Meanwhile, the O2 and O4 part of the uracil group had the high propensity to form hydrogen bonding with Thr263 and Arg238, respectively (Figure 7(d)). Both of the 3'-OH of the ribose also had high potency to form favorable hydrogen bonding interaction with Ser162 (3.8 and 2.8 Å, respectively) (Figure 7(b)). The phosphate groups could interact with Arg238 through hydrogen bonding and charge-charge interactions (Figure 7(d)). Hence, it might reveal the general interaction mode for five hSTING variants binding to **12g**. The docking data indicated that **12g** may interact with hSTING protein with high binding affinity. The ITC binding curves and ITC-based thermodynamic parameters for the complex formation of **12g** bound to hSTING-CTD protein were also recorded (Figure S13 and Table S2). The dissociation constants of **12g** bound to hSTING-WT-CTD and hSTING-R232H-CTD were $K_d=3.68$ and $6.75 \mu\text{M}$, separately. Both of the docking data and ITC test indicated that **12g** may interact with hSTING protein

Table 2 Dynamic calculation of the stacking interactions between the bases of CDNs with hSTING Y167 and R238 residues. Data counted a range of dihedral angle in $0\text{--}20^\circ$ and distance in $3.4\text{--}4 \text{ \AA}$

	Π_1	Π_2	Π_3	Π_4
9a	10,627	1,244	10,649	23
9b	1,009	1,922	14	1,883
9c	5	1	4,134	576
9d	8,339	142	9,912	3,028
9e	124 (A)	1,150(A)	10,494(G)	308(G)
16e	9,871(G)	700(G)	920(A)	6,527(A)

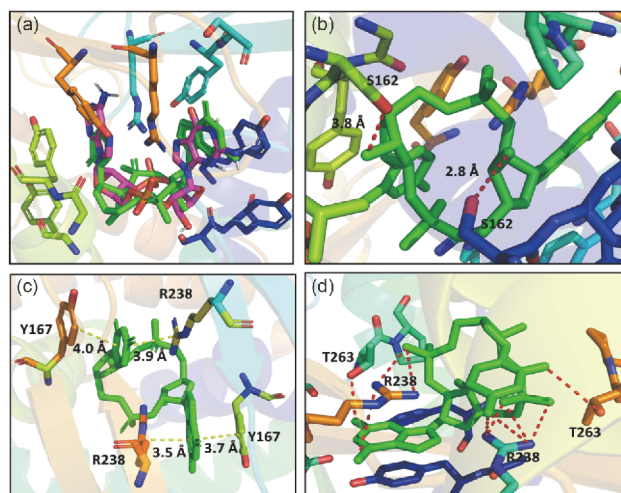


Figure 7 Docking calculation of **12g** and hSTING-R232H (aa 139–379). **12g** marked in green and **16e** marked in magenta (color online).

with high binding affinity.

The activity of CDNs inducing IFN- β production in THP-1 cells was also studied. THP-1-lucia cells were incubated in a culture media containing $10 \mu\text{M}$ of CDNs without any transfection reagents for 24 h. The IFN- β production activity was measured through luciferase reporter activity (Figure S14). CDNs constructed by G and A bases (**9e**, **12e**, **16e** and **16f**) could activate IFN- β induction dramatically. And the endogenous **16e** showed the highest activation activity. Cells did not give responses of IFN- β induction to CDNs with mixed pyrimidine except **12g**. It indicated that **12g** could activate IFN- β induction both in HEK293T (pre-transduced with hSTING) and THP-1 cell lines.

3.3 Stability of CDNs in serum and hydrolase

To achieve the long-lasting efficiency of CDNs for clinical applications, the serum stability and hydrolase stability of CDNs were indispensable. CDNs were constructed by two internucleotide phosphodiester bonds, which might be rapidly hydrolyzed by specific enzymes in serum. The instability in serum could restrict their *in vivo* potency. As reported, the only hydrolase called ENPP1 was proven to degrade **16e** in cultured cells while it was still unknown whether CDNs with other structures could be also degraded by ENPP1 [44,45]. Hence, we here intended to determine the stability of CDNs both in serum and ENPP1 solutions by HPLC.

After time-scale determination of the changes of CDNs in 10 mM phosphate buffer saline (PBS) buffer (pH 7.4) containing 20% FBS and 1 mM Mg^{2+} , we found that 3'-3' CDNs with two 3'-5' linkages ($T_{1/2}>50 \text{ h}$) were more stable than 2'-2' CDNs with two 2'-5' linkages ($T_{1/2}=6\text{--}20 \text{ h}$) and 2'-3' CDNs with one 3'-5' linkage and one 2'-5' linkage ($T_{1/2}=20\text{--}40 \text{ h}$) (Figure 8(a)). The results of the incubation of CDNs in ENPP1 were shown in Figure 8(b). CDNs with two 3'-5' linkages were more stable than CDNs with 2'-5' linkage while no significant difference between 2'-3' CDNs with one 2'-5' and one 3'-5' phosphodiester bond and 2'-2' CDNs with two 2'-5' phosphodiester bonds was observed. When CDNs were treated with ENPP1 (2 nM) for 48 h, 80% of 3'-3' CDNs were not degraded but only less than 20% of 2'-2' CDNs and 2'-3' CDNs were left, which was consistent with the stability assay in serum. Overall, the 3'-3' CDNs with two 3'-5' linkages provided a more hydrolase-resistant conformation. Contrary to expectations, **16a** and **12b** did not show much degradation in 72 h. This may be caused by the substrate selectivity of the catalytic pocket of ENPP1.

To further confirm that the degradation of CDNs was caused by hydrolase, we also identified that the CDNs in water could be stable for more than a month at room temperature. Through the calculation and NMR tests, we proposed that the 2'-5' phosphodiester linked ribose preferred

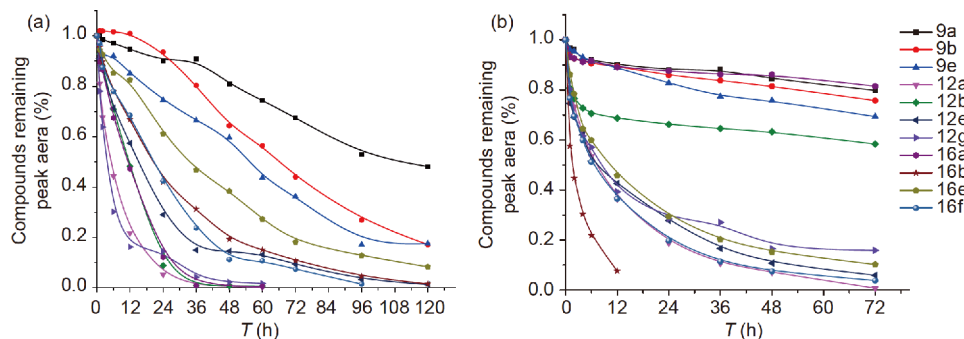


Figure 8 Time-scale HPLC analysis of CDNs in (a) 20% FBS and (b) 2 nM ENPP1 (color online).

the C2'-endolike (south-type) conformation and the 3'-5' phosphodiester linked ribose preferred C3'-endolike (north-type) conformation (Figure S12(a)) [25,33,46]. The special structure might endow CDNs the non-specific nuclease resistance. Based on the crystal-structure of ENPP1 in complex with **9e** obtained by Nureki *et al.* [44], they proposed that the ENPP1 favors to cleave the 2'-5' phosphodiester of **16e** in a conformation suitable for catalysis reaction instead of 3'-5' phosphodiester (Figure S12(b)), which was in accordance with our findings. The **16e** and **12g** showed the same stability in ENPP1. But **16e** ($T_{1/2}$ ~30 h) showed more stable than **12g** ($T_{1/2}$ less than 12 h) in serum. **16e** contains one 3'-5' phosphodiester bond and one 2'-5' phosphodiester bond and **12g** contains two 2'-5' phosphodiester bonds. According to the cell-based activity, the two CDNs showed same IFN- β induction level in HEK293T cell with transduction of hSTING R232H and AQ. However, HEK293T cells expressing hSTING-WT, HAQ and R293Q, **16e** showed higher activity than **12g**. When **16e** and **12g** were transfected into THP-1 cells through co-incubation in serum-containing culture media, **16e** also showed much higher activity than **12g**. The higher stability of **16e** may also contribute the higher activity.

In summary, CDNs with two 3'-5' phosphodiester linkage were more stable than CDNs with one or two 2'-5' phosphodiester linkages in serum and ENPP1, and the base type in CDNs contributed little to the stability of CDNs. However, depending on the IFN- β -induction results, CDNs with 2'-5' phosphodiester linkage had more potency to activate hSTING, especially for the mixed pyrimidine CDNs. Taken together, in order to balance the activity and stability of CDNs, these results suggested that a more stable 2'-5' phosphodiester substitution would be better suited to the clinical application.

4 Conclusions

Cyclic dinucleotides (CDNs) have been recognized as important secondary messengers both in prokaryotes and eukaryotes recently. For the first time, all possible (a total of

36) CDNs that containing four natural bases (A, G, C, U) and two linkage directions (2'-5'-linked and 3'-5'-linked phosphodiester) have herein been synthesized and evaluated against all five hSTING SNPs reported so far. Surprisingly, we have found for the first time that c[G(2',5')U(2',5')] has expressed excellent activation activity toward IFN- β induction on all five hSTING variants, comparable to c[G(2',5')A(3',5')]. The serum stability screen by serum/ENPP1 hydrolyase has shown that 3'-3' analogues showed more stable than 2'-3' and 2'-2' analogues. Our results showed that different CDNs activate all five hSTING protein variants differently, normally with lower activity against hSTING-R232H and hSTING-R293Q. It is very interesting to note that three distinctive phosphodiester linkage types (3'-3', 2'-3', 2'-2') all yield purine-purine CDNs with good activity, but only c[G(2',5')U(2',5')] showing excellent activation activity against all five hSTING mutants. Our docking study showed that the Tyr167 and Arg238 of hSTING may provide the stacking interaction with Uracil to enhance the CDN activation. Until now, 3'-3' CDNs such as c[G(3',5')G(3',5')], c[A(3',5')A(3',5')], c[G(3',5')A(3',5')] and c[A(3',5')U(3',5')] were discovered in bacteria and 2'-3' CDNs such as c[G(2',5')A(3',5')] regulates immune system in mammalian. However, 2'-2' CDNs are not found yet in natural sources. What is more, no CDNs are found in the plant yet. It causes our great interests in founding whether CDNs, especially the 2'-2' CDNs, could also play as second messengers in the plant to regulate part of physiological bioactivities. Further study is ongoing to gain our understanding on the mechanism.

Acknowledgements This work was supported by the National Key Research and Development Program of China (2017YFD0200500) and the National Natural Science Foundation of China (21740002, 21837001). We also thanks Prof. Junmin Quan for the support of THP-1-Lucia cells and Prof. Dongsheng Guo for the help of ITC assay.

Conflict of interest The authors declare that they have no conflict of interest.

Supporting information The supporting information is available online at <http://chem.scichina.com> and <http://link.springer.com/journal/11426>. The

supporting materials are published as submitted, without typesetting or editing. The responsibility for scientific accuracy and content remains entirely with the authors.

- Krasteva PV, Sondermann H. *Nat Chem Biol*, 2017, 13: 350–359
- Schaap P. *IUBMB Life*, 2013, 65: 897–903
- Sun L, Wu J, Du F, Chen X, Chen ZJ. *Science*, 2013, 339: 786–791
- Wu J, Sun L, Chen X, Du F, Shi H, Chen C, Chen ZJ. *Science*, 2013, 339: 826–830
- Gao P, Ascano M, Zillinger T, Wang W, Dai P, Serganov AA, Gaffney BL, Shuman S, Jones RA, Deng L, Hartmann G, Barchet W, Tuschl T, Patel DJ. *Cell*, 2013, 154: 748–762
- Zhang X, Shi H, Wu J, Zhang X, Sun L, Chen C, Chen ZJ. *Mol Cell*, 2013, 51: 226–235
- Ablasser A, Goldeck M, Cavlar T, Deimling T, Witte G, Röhl I, Hopfner KP, Ludwig J, Hornung V. *Nature*, 2013, 498: 380–384
- Lioux T, Mauny MA, Lamoureux A, Bascoul N, Hays M, Vernejoul F, Baudru AS, Boullaran C, Lopes-Vicente J, Qushair G, Tirabay G. *J Med Chem*, 2016, 59: 10253–10267
- Burdette DL, Monroe KM, Sotelo-Troha K, Iwig JS, Eckert B, Hyodo M, Hayakawa Y, Vance RE. *Nature*, 2011, 478: 515–518
- Shi H, Wu J, Chen ZJ, Chen C. *Proc Natl Acad Sci USA*, 2015, 112: 8947–8952
- Wang C, Sinn M, Stifel J, Heiler AC, Sommershof A, Hartig JS. *J Am Chem Soc*, 2017, 139: 16154–16160
- Fu J, Kanne DB, Leong M, Glickman LH, McWhirter SM, Lemmens E, Mechette K, Leong JJ, Lauer P, Liu W, Sivick KE, Zeng Q, Soares KC, Zheng L, Portnoy DA, Woodward JJ, Pardoll DM, Dubensky Jr. TW, Kim Y. *Sci Transl Med*, 2015, 7: 283ra52
- Ghaffari A, Peterson N, Khalaj K, Vitkin N, Robinson A, Francis JA, Koti M. *Br J Cancer*, 2018, 119: 440–449
- Wang H, Hu S, Chen X, Shi H, Chen C, Sun L, Chen ZJ. *Proc Natl Acad Sci USA*, 2017, 114: 1637–1642
- Smith TT, Moffett HF, Stephan SB, Opel CF, Dumigan AG, Jiang X, Pillarisetty VG, Pillai SPS, Wittrop KD, Stephan MT. *J Clin Invest*, 2017, 127: 2176–2191
- Deng L, Liang H, Xu M, Yang X, Burnette B, Arina A, Li XD, Mauerci H, Beckett M, Darga T, Huang X, Gajewski TF, Chen ZJ, Fu YX, Weichselbaum RR. *Immunity*, 2014, 41: 843–852
- Li T, Cheng H, Yuan H, Xu Q, Shu C, Zhang Y, Xu P, Tan J, Rui Y, Li P, Tan X. *Sci Rep*, 2016, 6: 19049
- Yi G, Brendel VP, Shu C, Li P, Palanathan S, Cheng Kao C. *PLoS ONE*, 2013, 8: e77846
- Whiteley AT, Eaglesham JB, de Oliveira Mann CC, Morehouse BR, Lowey B, Nieminen EA, Danilchanka O, King DS, Lee ASY, Mekanalos JJ, Kranzusch PJ. *Nature*, 2019, 567: 194–199
- Gentili M, Kowal J, Tkach M, Satoh T, Lahaye X, Conrad C, Boyron M, Lombard B, Durand S, Kroemer G, Loew D, Dalod M, Théry C, Manel N. *Science*, 2015, 349: 1232–1236
- Girardin SE, Boneca IG, Carneiro LAM, Antignac A, Jéhanno M, Viala J, Tedin K, Taha MK, Labigne A, Zähringer U, Coyle AJ, DiStefano PS, Bertin J, Sansonetti PJ, Philpott DJ. *Science*, 2003, 300: 1584–1587
- Case DA, Case D, Berryman J, Betz RM, Cerutti DS, Cheatham T, Darden T, Duke RE, Giese TJ, Gohlke H, Götz A, Homeyer N, Izadi S, Janowski P, Kaus J, Kovalenko A, Lee TS, LeGrand S, Li P, Luchko T, Kollman PA. *Amber 2015, University of California, San Francisco*, 2015
- Salomon-Ferrer R, Götz AW, Poole D, Le Grand S, Walker RC. *J Chem Theor Comput*, 2013, 9: 3878–3888
- Maier JA, Martinez C, Kasavajhala K, Wickstrom L, Hauser KE, Simmerling C. *J Chem Theor Comput*, 2015, 11: 3696–3713
- Wang B, Wang Z, Javornik U, Xi Z, Plavec J. *Sci Rep*, 2017, 7: 16550
- Darden T, York D, Pedersen L. *J Chem Phys*, 1993, 98: 10089–10092
- Ryckaert JP, Ciccotti G, Berendsen HJC. *J Comput Phys*, 1997, 23: 327–341
- Zhang C, Shang G, Gui X, Zhang X, Bai XC, Chen ZJ. *Nature*, 2019, 567: 394–398
- Zhao B, Du F, Xu P, Shu C, Sankaran B, Bell SL, Liu M, Lei Y, Gao X, Fu X, Zhu F, Liu Y, Laganowsky A, Zheng X, Ji JY, West AP, Watson RO, Li P. *Nature*, 2019, 569: 718–722
- Mukai K, Konno H, Akiba T, Uemura T, Waguri S, Kobayashi T, Barber GN, Arai H, Taguchi T. *Nat Commun*, 2016, 7: 11932
- Corrales L, Glickman LH, McWhirter SM, Kanne DB, Sivick KE, Katibah GE, Woo SR, Lemmens E, Banda T, Leong JJ, Metchette K, Dubensky Jr. TW, Gajewski TF. *Cell Rep*, 2015, 11: 1018–1030
- Yin Q, Tian Y, Kabaleeswaran V, Jiang X, Tu D, Eck MJ, Chen ZJ, Wu H. *Mol Cell*, 2012, 46: 735–745
- Che X, Zhang J, Quan H, Yang L, Gao YQ. *J Phys Chem B*, 2018, 122: 1862–1868
- Volpi S, Insalaco A, Caorsi R, Santori E, Messia V, Sacco O, Terheggen-Lagro S, Cardinale F, Scarselli A, Pastorino C, Moneta G, Cangemi G, Passarelli C, Ricci M, Girosi D, Derchi M, Bocca P, Diociaiuti A, El Hachem M, Cancrini C, Tomà P, Granata C, Ravelli A, Candotti F, Picco P, DeBenedetti F, Gattorno M. *J Clin Immunol*, 2019, 39: 476–485
- Motwani M, Pawaria S, Bernier J, Moses S, Henry K, Fang T, Burkly L, Marshak-Rothstein A, Fitzgerald KA. *Proc Natl Acad Sci USA*, 2019, 116: 7941–7950
- Konno H, Chinn IK, Hong D, Orange JS, Lupski JR, Mendoza A, Pedrosa LA, Barber GN. *Cell Rep*, 2018, 23: 1112–1123
- Melki I, Rose Y, Ugenti C, Van Eyck L, Frémond ML, Kitabayashi N, Rice GI, Jenkinson EM, Boulai A, Jeremiah N, Gattorno M, Volpi S, Sacco O, Terheggen-Lagro SWJ, Tiddens HAWM, Meyts I, Morren MA, De Haes P, Wouters C, Legius E, Corveleyn A, Rieux-Laucat F, Bodemer C, Callebaut I, Rodero MP, Crow YJ. *J Allergy Clin Immunol*, 2017, 140: 543–552.e5
- Huang YH, Liu XY, Du XX, Jiang ZF, Su XD. *Nat Struct Mol Biol*, 2012, 19: 728–730
- Shang G, Zhu D, Li N, Zhang J, Zhu C, Lu D, Liu C, Yu Q, Zhao Y, Xu S, Gu L. *Nat Struct Mol Biol*, 2012, 19: 725–727
- Shu C, Yi G, Watts T, Kao CC, Li P. *Nat Struct Mol Biol*, 2012, 19: 722–724
- Shang G, Zhang C, Chen ZJ, Bai XC, Zhang X. *Nature*, 2019, 567: 389–393
- Ouyang S, Song X, Wang Y, Ru H, Shaw N, Jiang Y, Niu F, Zhu Y, Qiu W, Parvatiyar K, Li Y, Zhang R, Cheng G, Liu ZJ. *Immunity*, 2012, 36: 1073–1086
- Ergun SL, Fernandez D, Weiss TM, Li L. *Cell*, 2019, 178: 290–301.e10
- Kato K, Nishimasu H, Oikawa D, Hirano S, Hirano H, Kasuya G, Ishitani R, Tokunaga F, Nureki O. *Nat Commun*, 2018, 9: 4424
- Li L, Yin Q, Kuss P, Maliga Z, Millán JL, Wu H, Mitchison TJ. *Nat Chem Biol*, 2014, 10: 1043–1048
- Che X, Zhang J, Zhu Y, Yang L, Quan H, Gao YQ. *J Phys Chem B*, 2016, 120: 2670–2680